Oxidation of Tetrahydrostilbazole by Monoamine Oxidase A Demonstrates the Effect of Alternate Pathways in the Kinetic Mechanism†

Rona R. Ramsay,*,‡ Sergey O. Sablin,‡ Sergey O. Bachurin,§ and Thomas P. Singer‡,∥

Department of Biochemistry and Biophysics and Division of Toxicology, University of California at San Francisco, San Francisco, California 94143, Molecular Biology Division, Department of Veterans Affairs Medical Center, 4150 Clement Street, San Francisco, California 94121, and Institute of Physiologically Active Substances, Russian Academy of Sciences, 142432 Chernogolovka, Moscow Region, Russia

Received January 27, 1993; Revised Manuscript Received April 9, 1993

ABSTRACT: The steady-state kinetics for the oxidation of 1-methyl-1,2,3,6-tetrahydrostilbazole (MTHS) by purified human liver monoamine oxidase A yielded biphasic double-reciprocal plots. Rate constants from stopped-flow studies were determined to show that the apparent stimulation at high substrate concentrations can be explained in terms of the alternate oxidative pathways available to monoamine oxidase A [Ramsay, R. R. (1991) *Biochemistry 30,* 4624–4629]. At low substrate concentrations, the slower reoxidation of the free enzyme (second-order rate constant was 4000 M^{-1} s^{-1}) predominates, but at higher concentrations the faster reoxidation of the reduced enzyme–substrate complex (38 300 M^{-1} s^{-1}) becomes significant. Computer simulation using this model predicts that similar biphasic curves could be obtained for the oxidation of the neurotoxin, 1-methyl-4-phenyl-1,2,3,6-tetrahydropyridine, but that nonlinearity would be obvious only at concentrations above $200K_m$.

Monoamine oxidases A and B oxidize neuroactive and vasoactive amines in the brain and in peripheral tissues. Although both enzymes oxidize primary, secondary, and tertiary amines, their substrate and inhibitor specificities differ [reviewed by Singer (1991)]. A wide range of substrates and their analogs have been used to investigate the topography of the active sites to identify the differences between the two forms of the enzyme. Considerable progress toward this end has been made on the basis of structure–activity data for analogs of the neurotoxin MPTP[1] (Youngster *et al.*, 1989; Efange & Boudreau, 1991; Altomare *et al.*, 1992). The reaction catalyzed by MAO necessitates the interaction of the substrate site and flavin for the oxidation of the amine with concomitant reduction of the flavin. The reduced flavin is reoxidized by molecular oxygen which may, by analogy with other flavoenzymes, include the formation of a C-4a hydroperoxyflavin derivative (Massey *et al.*, 1988). The site of O_2 binding to the enzyme must be considered as a second substrate site. As yet, nothing is known about this site in MAO, its relationship to the amine binding site, or the relationship of either of these sites to the flavin.

Kinetic studies indicate that amine binding influences the reaction of the reduced flavin with oxygen (Ramsay *et al.*, 1987; Ramsay, 1991). The enhancement of the reactivity with oxygen depends on the nature of the amine substrate and is much greater in MAO A than in MAO B (Ramsay *et al.*, 1992; Tan & Ramsay, 1993). The steady-state and half-reaction data on which these observations were based can be explained by alternate pathways for the oxidation of the reduced flavin in MAO. Free reduced enzyme is oxidized slowly, but reduced enzyme with the amine substrate (not product) bound is reoxidized many times more rapidly. The affinity of the reduced enzyme for the amine is not necessarily the same as that of the oxidized enzyme. Thus, the flux through each branch depends on the level of free reduced enzyme and on the affinity of the amine for the reduced enzyme, together with the relative rates in the two branches (Tan & Ramsay, 1993).

1-Methyl-1,2,3,6-tetrahydrostilbazole (MTHS) and its analogs have been studied as substrates of both forms of MAO (Sablin *et al.*, 1990). It was shown that a partially purified preparation from pig liver which contained both MAO A and B catalyzed the slow oxidiation of MTHS and its analogs with kinetics characterized by two pairs of parameters. Since no selective inhibitor of MAO A or B, such as clorgyline or deprenyl, was used in the assays, it was not possible to decide what part of the activity could be attributed to either enzyme. We decided to reinvestigate the oxidation of MTHS analogs by highly purified MAO A and MAO B. In the course of this study it was noted that although the reaction with MAO B showed linear kinetic behavior, MAO A gave biphasic Lineweaver–Burk plots. This paper explores the reasons for the nonlinear kinetics and demonstrates that these observations can be explained in terms of the alternate mechanisms for the reoxidation of the reduced enzyme.

MATERIALS AND METHODS

Human liver monoamine oxidase A expressed in yeast was purified as described by Tan *et al.* (1991). Before use, the enzyme was dialyzed against 50 mM sodium phosphate, pH 7.2, containing 0.8% (w/v) *n*-octyl β-D-glucopyranoside. Steady-state kinetics were determined in 50 mM sodium phosphate, pH 7.2, at 30 °C in a Hitachi U2000 spectrophotometer equipped with a thermostated six-cell changer and computerized data collection. The rate of production of methyldihydrostilbazole (the dihydropyridinium product) was

† This research was supported by the National Institutes of Health (HL-16251), by the National Science Foundation (DMB-9020015), and by the Department of Veterans Affairs.

* Address correspondence to this author at the Molecular Biology Division, 151-S, Veterans Administration Medical Center, 4150 Clement St., San Francisco, CA 94121 [telephone (415) 752-9676; fax (415) 750-6959].

‡ University of California.

§ Russian Academy of Sciences.

∥ Department of Veterans Affairs Medical Center.

[1] Abbreviations: MPTP, 1-methyl-4-phenyl-1,2,3,6-tetrahydropyridine; MAO, monoamine oxidase; MTHS, 1-methyl-1,2,3,6-tetrahydrostilbazole.

0006-2960/93/0432-9025$04.00/0

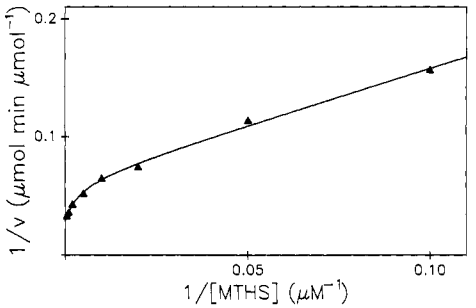

FIGURE 1: Steady-state kinetics for the oxidation of MTHS by monoamine oxidase A. The appearance of 2,3-dihydropyridinium product was followed spectrophotometrically at 383 nm. The assay mixture contained 50 mM sodium phosphate, pH 7.2, equilibrated with air at 30 °C, and enzyme (50 nM). The reaction was initiated by addition of MTHS. The velocity is expressed in micromoles of product per minute per micromole of enzyme flavin in the assay, which is equivalent to the turnover number (min^{-1}).

measured at 383 nm, where the extinction coefficient is 24 mM^{-1} cm^{-1} (Sablin, 1991). Stopped-flow experiments were conducted as described before (Ramsay *et al.*, 1987; Ramsay, 1991), except that the changes in the absorbance of the flavin were followed at 490 nm to avoid interference from the absorption of the dihydropyridinium [ϵ(450 nm) = 1.1 mM^{-1} cm^{-1}]. For the reductive half-reaction, reduction was also measured by following the appearance of the dihydropyridinium product at 370 nm to extend the range of substrate concentrations down to 15 μM and still satisfy the requirement [S] $\gg$ [E]. The extinction coefficient of methyldihydrostilbazole at 370 nm is 21 mM^{-1} cm^{-1} (Sablin, 1991). At 2 μM enzyme concentration, the net absorbance change in the stopped-flow experiments was 0.036, as expected from the difference extinction coefficient of 18 mM^{-1} cm^{-1} calculated by correcting the methyldihydrostilbazole extinction coefficient for the decrease in the absorbance of the flavin at that wavelength.

MTHS was provided by Mr. S. E. Tkachenko, Institute of Physiologically Active Substances, Russian Academy of Sciences, Chernogolovka, Moscow Region, Russia. The purity and identity were confirmed by elemental analysis, MS, and NMR. Details of the synthesis will be published elsewhere. MTHS is potentially neurotoxic, so aerosols and skin contact were avoided.

The Runge simulation program (Anarac Associates, San Diego, CA) was the gift of Dr. Steven C. Koerber. The simulation of Scheme II used another program for modeling kinetic systems, written by Dr. Vladislav V. Kuusk, Molecular Biology Division, VAMC 151-S, 4150 Clement St., San Francisco, CA 94121.

RESULTS

Steady-State Kinetics. The oxidation of *trans*-MTHS catalyzed by MAO A yields nonlinear double-reciprocal plots when the range of substrate concentrations is sufficiently wide (Figure 1). At low concentrations of MTHS (<100 μM), the reaction is extremely slow, with an estimated V_{max} (expressed as the turnover number per flavin) of 0.15 s^{-1}. For comparison, that for MPTP is 0.2 s^{-1} and that for kynuramine is 2.6 s^{-1} (Ramsay, 1991). At concentrations of MTHS above 200 μM there is a sharp, apparent activation of the enzyme to give the higher V_{max} of 0.6 s^{-1}. The data shown in Figure 1 were fitted to a simple two-site model to obtain the K_m values given in Table I. These are complex kinetic parameters and cannot be taken as estimates of K_s. To estimate how well MTHS binds to the enzyme, we determined the K_i for the inhibition of kynuramine oxidation by MTHS. Figure 2 shows the

Table I: Kinetic Parameters for the Oxidation of MTHS by MAO A from Steady-State and Pre-Steady-State Half-Reaction Experiments

	turnover no. (s^{-1})	K_{m1}[a] (μM)	K_{m2}[a] (μM)
steady state[b]	0.58	10	400
	k_3 (s^{-1})		$K_D(E_{OX}S)$ (μM)
reduction[c]	0.045		3.2
oxidation	app first-order k' (s^{-1})	app second-order k (M^{-1} s^{-1})	$K_D(E_RS)$ (μM)
free enzyme[d]	0.9	3 600	
ligand in enzyme[d]	8.9	37 300	6
ligand in O_2[e]	9.1	38 300	

[a] For convenient estimation the steady-state data were fitted to a double hyperbola which describes the data in terms of two binding sites: $V_1K_{m1}/(K_{m1}+S) + V_2K_{m2}/(K_{m2}+S)$. [b] From Figure 1. [c] From Figure 4. [d] From Figure 5. [e] From Figure 6. [f] At air saturation.

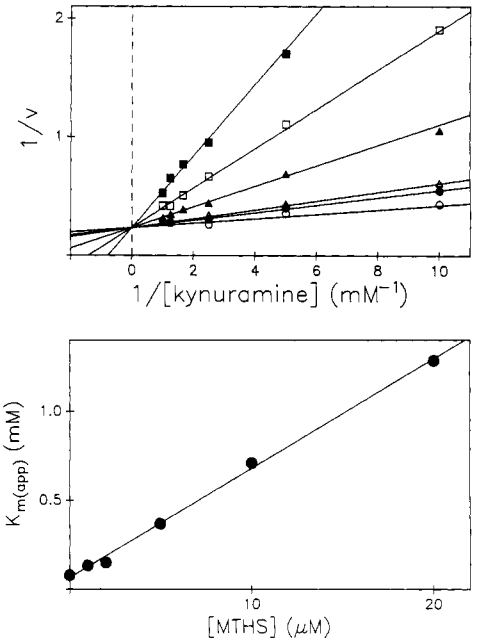

FIGURE 2: MTHS competitively inhibits the oxidation of kynuramine by MAO A. (A, top) Lineweaver–Burk plot of the inhibition of kynuramine oxidation by MTHS when kynuramine was the varied substrate and when only the product of kynuramine oxidation was measured spectrophotometrically at 316 nm. The assay mixture contained 50 mM sodium phosphate buffer, pH 7.2, and 35 nM MAO A. Amounts of MTHS were (○) 0, (●) 1, (△) 2, (▲) 5, (□) 10, and (■) 20 μM. Rates of oxidation are expressed in micromoles of product formed per minute per 1-mL assay. (B, bottom) Secondary plot of the apparent K_m values from (A).

competitive inhibition by the slow substrate. The K_i is 2 μM. To confirm that the rapid equilibrium assumption could be made for inhibitor binding, the experiment was done in two ways. In one, the enzyme was preincubated with MTHS for 5 min before addition of kynuramine. In the other, the reaction was initiated by addition of the enzyme to the cuvette with both kynuramine and MTHS present. No difference in the inhibition of kynuramine oxidation by MTHS was found between these two protocols.

Low concentrations of MTHS were used to examine the dependence on the oxygen concentration (Figure 3). The K_m for oxygen obtained under these conditions was estimated to be 10 μM from Figure 3, lower than that found when kynuramine was the amine substrate (60 μM; Ramsay *et al.*, 1992). When concentrations of MTHS above 200 μM were

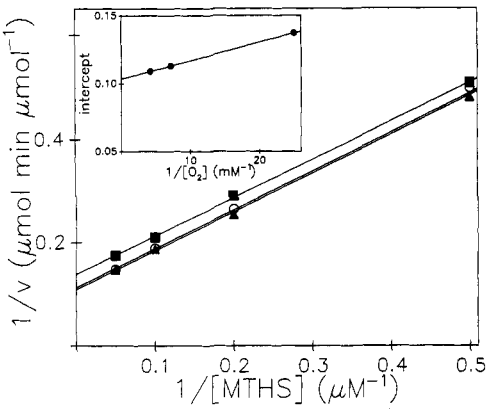

FIGURE 3: Oxygen dependence of the initial steady-state rates at low MTHS concentrations. The assay is described in Figure 2. The oxygen concentrations were (■) 0.04, (○) 0.14, and (▲) 0.238 mM. (Main panel) Double-reciprocal plot; (inset) secondary plot of the $1/V_{max}$ intercepts from (A).

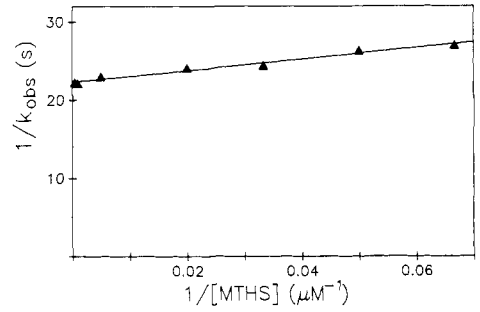

FIGURE 4: Double-reciprocal plot for the dependence of observed rate constant for reduction of monoamine oxidase A on the concentration of MTHS is linear. The rates of reductive half-reaction were measured at 30 °C, as described under Materials and Methods. The reaction mixture contained 2 μM enzyme, 50 mM sodium phosphate, pH 7.2, 30 mM glucose, 1 unit/mL glucose oxidase, 24 unit/mL catalase, and substrate as indicated.

used, varying the oxygen concentration had so little effect on the observed initial rates that the K_m could not be determined.

To seek an explanation for the curved double-reciprocal plot, we determined the rate constants for the half-reactions by the stopped-flow method.

Reductive Half-Reaction of MAO A with MTHS. To determine the rate of the reductive half-reaction, which has been found to be the rate-determining step for MAO A with all substrates examined so far (Tan & Ramsay, 1993), oxidized enzyme was mixed with excess substrate under anaerobic conditions and the bleaching of the flavin followed at 490 nm (instead of 450 nm, where the tail absorption of the dihydropyridinium product of MTHS interferes). The reduction of MAO A by MTHS proceeded very slowly, following pseudo-first-order kinetics, and showed a simple dependence on the substrate concentration. Despite the steady-state observations, the double-reciprocal plot of the rate constant for the reductive half-reaction vs a wide range of concentrations of MTHS (0.1–2 mM) was linear (not shown). However, in steady-state experiments, the K_i for MTHS (with kynuramine as substrate) was only 2 μM and the low K_m estimated from steady state was 10 μM, concentrations too low to investigate by this method for which the enzyme concentration must be around 10 μM. To get closer to the desired substrate range, the enzyme concentration was decreased to 2 μM and the rate of appearance of the product followed at 370 nm (net extinction coefficient 18 mM^{-1} cm^{-1}). The double-reciprocal plot was linear from 0.015 to 2 mM MTHS (Figure 4) and was identical to that obtained by monitoring the flavin reduction. From Figure 4, the rate constant for the reduction of the flavin in

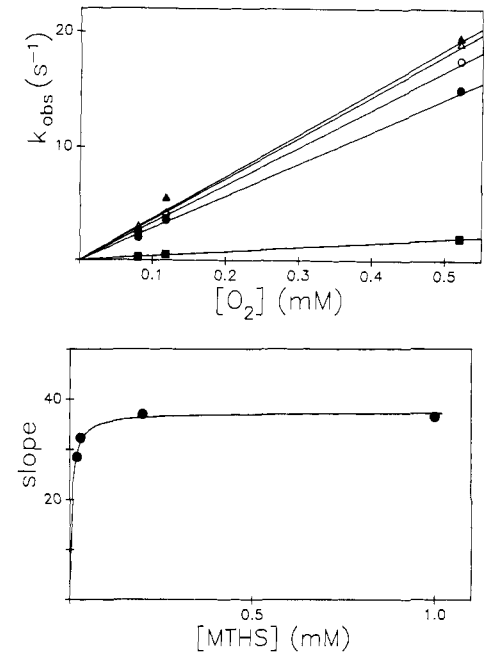

FIGURE 5: MTHS preincubated with enzyme stimulates the reoxidation of reduced monoamine oxidase A. (A, top) Reduced monoamine oxidase A (10 μM) was premixed anaerobically with MTHS in the stopped-flow syringe and incubated for 5 min at 30 °C before oxidation was initiated by mixing with the oxygenated buffer containing the same concentration of MTHS. The increase in absorbance at 430 nm was recorded. The MTHS concentrations were (■) 0, (●) 0.02, (○) 0.03, (▲) 0.2, and (△) 1 mM. (B, bottom) Secondary plot of the slopes from (A).

the enzyme–substrate complex (k_3; the rate constants are assigned as shown in Scheme II) and the dissociation constant for that complex, $K_D(E_{OX}S)$, can be calculated (Table I). Similar linear plots were obtained for other substrates with MAO A, such as kynuramine and serotonin but, for MPTP, which is structurally closest to MTHS, the double-reciprocal plot curved upward at higher abcissa values, indicating that k_3 was comparable to k_2, the rate constant for dissociation of the $E_{OX}S$ complex (Ramsay, 1991; Tan & Ramsay, 1993). For MTHS, k_2 and k_3 must be different since the double-reciprocal plot is linear (Figure 4). The k_3 calculated for MTHS is extremely low (0.04 s^{-1}, Table I), so it is likely that k_2 is very much larger. Curiously, the k_3 value of 0.04 s^{-1} is very much less than the steady-state turnover number of 0.6 s^{-1} (Table I). Since the overall reaction cannot be faster than the slowest step, this discrepancy indicates either that there is an alternate path to the $E_{OX}S \rightarrow E_RP$ step under turnover conditions or that the presence of oxygen of alters the rate of reduction. The lack of anomalies due to the high concentration of enzyme used in the stopped-flow method on the kinetic parameters was documented for MAO B oxidizing benzylamine (Husain *et al.*, 1982). The steady-state parmeters for MAO A with MTHS were redetermined at high (0.2 μM) enzyme concentration and found to be the same as those in Table I. Thus, the turnover number is independent of the enzyme concentration and the discrepancy between k_3 and turnover number is unlikely to arise from the higher enzyme concentration used in the stopped-flow experiments.

Oxidative Half-Reaction. The effect of MTHS on the reoxidation of reduced MAO A was examined to determine the rate constant for the reoxidation of the E_RS complex. All substrates tested so far stimulate the rate of reaction of reduced MAO A with oxygen (Tan & Ramsay, 1993). Figure 5 shows that MTHS is no exception. MAO reduced by the xanthine oxidase method (Ramsay, 1991; Massey, 1991) was preincubated anaerobically with MTHS for 5 min before mixing

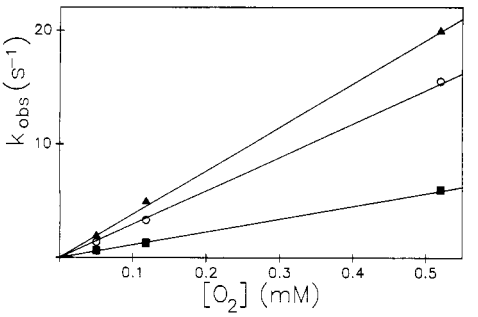

FIGURE 6: MTHS mixed with reduced monoamine oxidase A at the same time as oxygen also stimulates the rate of reoxidation. Reduced monoamine oxidase (6.5 μM) was mixed in the stopped-flow spectrophotometer with oxygenated buffer containing (■) 0.05, (○) 0.2, and (▲) 7 mM MTHS.

with O_2 in the stopped-flow chamber. In the absence of substrate, reoxidation of the free reduced enzyme is a bimolecular process with a second-order rate constant of 4000 M^{-1} s^{-1}. In the presence of MTHS, the rate of reoxidation is increased but all lines still go through the origin (Figure 5A). The increase in rate is dependent on the substrate concentration, suggesting that the observed rate depends not only on the reaction of E_RS with O_2 but also on the $E_R + S \rightleftharpoons E_RS$ equilibrium. Thus, in contrast to the experiments with other substrates (Ramsay, 1991; Tan & Ramsay, 1993), these data permit the calculation of an apparent binding constant for the effect of MTHS on the reoxidation. The K_D for E_RS estimated from Figure 5B is 6 μM, very close to the K_D for $E_{OX}S$ (3 μM, see Table I). However, comparison of Figures 5A and 6 reveals that the same concentration of MTHS gives quite different lines depending on whether or not the reduced enzyme is preincubated with MTHS prior to mixing with O_2. Without premixing, the equilibrium of $E_R + S \rightleftharpoons E_RS$ is not reached before oxidation is complete. Thus, the on-rate for substrate binding (k_4[S]) must be comparable to k_5[O_2]. The off-rate (k_{-4}) must be slower, since very little dissociates before oxidation is complete (Figure 5A). When the substrate is premixed with the enzyme, the maximum rate of oxidation is seen except at the very lowest MTHS concentration. Thus, in Figure 5A most of the enzyme is reoxidized via the E_RS path when MTHS is present, whereas in the experiment shown in Figure 6, much of it is reoxidized via the E_R path, especially at low MTHS concentrations.

Simulations. To visualize the interplay of the two pathways of reoxidation under various experimental conditions, Scheme I was used to model the reaction using the Runge program, with the on- and off-rates (k_4 and k_{-4}) arbitrarily set at 1 s^{-1} and the other rate constants as in Table I (k_5 = 0.5 s^{-1}, k_6 = 5 s^{-1}) and [O_2] = 0.12 mM. At low substrate concentration ([MTHS] = 0.1 mM), free enzyme species predominate, but at high [MTHS] (10 mM), the enzyme–substrate complexes (EA) are the prevalent species (simulations not shown). If the rate of dissociation of E_RS (k_{-4}) is decreased, E_{RS} builds up and a larger proportion of the enzyme is oxidized via the enzyme–substrate complex. The effect of substrate concentration on the relative flux through the two oxidative pathways could in itself account for the stimulation of the observed rate in steady-state assays by high [MTHS], if the reoxidation of the reduced enzyme were rate-limiting in the kinetic mechanism. The maximum steady-state rate (0.6 s^{-1}) is indeed similar to the rate of reoxidation of the free enzyme (1 s^{-1} at air saturation). In light of the information on the reoxidative half-reaction, a likely explanation for the biphasic steady-state kinetics emerges. As a consequence of the branched pathway mechanism of MAO A in which substrate stimulates reoxidation and with the particular rate and binding constants

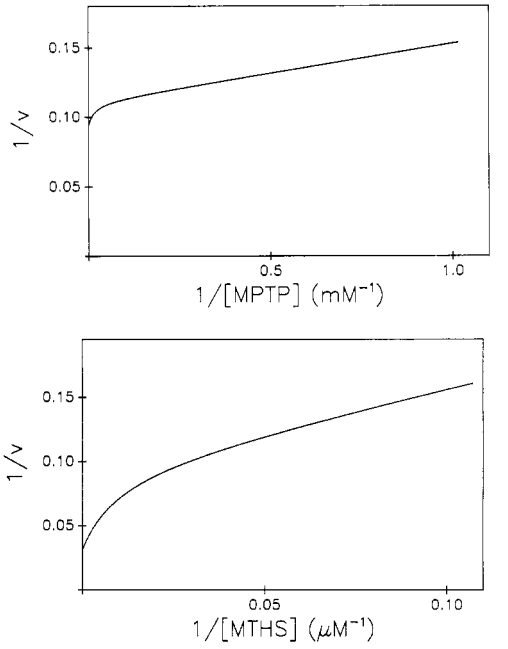

FIGURE 7: Theoretical curves generated from Scheme II with the program for modeling kinetic systems (see Materials and Methods). (A, top) Double-reciprocal plot for MPTP is also curved at very high substrate concentrations (>20 mM). Kinetic constants for the simulation based on Scheme IIA were taken from Ramsay (1991). The values used were $k_1 = 0.484 \times 10^{-3}$ μM^{-1} s^{-1}, k_2 = 0.038 s^{-1}, k_3 = 0.18 s^{-1}, $k_7 = 1 \times 10^{-5}$ μM^{-1} s^{-1}, $k_8 = 1 \times 10^{-4}$ s^{-1}, k_9 = 0.138 s^{-1}, and k_{10} = 0.004 μM^{-1} s^{-1}. The steady-state constants for the plot shown were V_1 = 0.18 s^{-1}, K_{m1} = 0.38 mM, and K_{m2} = 72 mM. (B, bottom) Double-reciprocal plot for MTHS. The kinetic constants (from Table I) were k_1 = 1 μM^{-1} s^{-1}, k_2 = 2 s^{-1}, k_3 = 0.045 s^{-1}, k_4 = 0.6 s^{-1}, k_5 = 0.001 s^{-1}, k_6 = 0.01 s^{-1}, k_7 = 0.3 μM^{-1} s^{-1}, k_8 = 1.8 s^{-1}, k_9 = 0.038 μM^{-1} s^{-1}, and k_{10} = 0.0036 μM^{-1} s^{-1}. When the data from a simulation using Scheme IIB were fitted to a double hyperbola as for Figure 1, the constants obtained were V = 0.54 s^{-1}, K_{m1} = 6 μM, and K_{m2} = 320 μM.

Scheme I: Model of the Alternate Oxidative Pathways Used To Predict the Distribution of Enzyme Species Shown in Figure 7

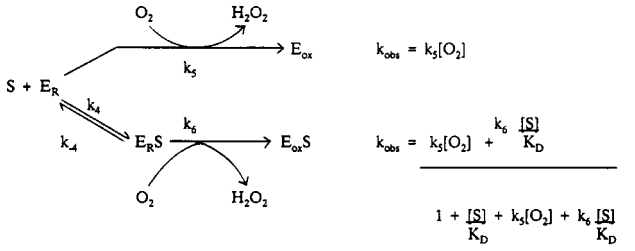

observed for the oxidation of MTHS, each branch of the pathway predominates at different substrate concentrations.

To begin to identify which steps in the mechanism are important in determining which branch (free enzyme or enzyme–substrate complex) predominates in the steady-state reaction, we also simulated the steady-state turnover based on the basic scheme as shown in Scheme IIA. Scheme IIA is the same as proposed previously (Ramsay, 1991) and is adequate to simulate the results obtained with substrates such as MPTP (Figure 7A). However, with MTHS the steady-state rate is 0.6 s^{-1}, but the rate constant calculated from stopped-flow experiments for the reductive half-reaction (k_3 in Scheme IIA) was only 0.04 s^{-1} (Table I). Simulations based on Scheme IIA gave curvature but correlated poorly with the observed data at low substrate concentrations. This discrepancy means that an isomerization step must be invoked in the description of the half-reaction so that the slow step can be bypassed during turnover. Scheme IIB proposes a modified

Scheme II: Minimal Model for the Steady-State Oxidation of MTHS by MAO A

A.

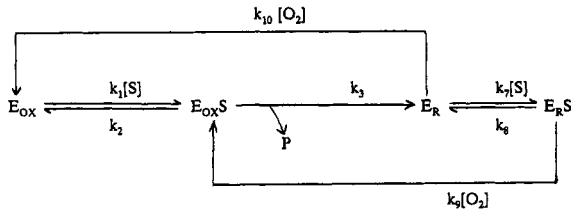

B.

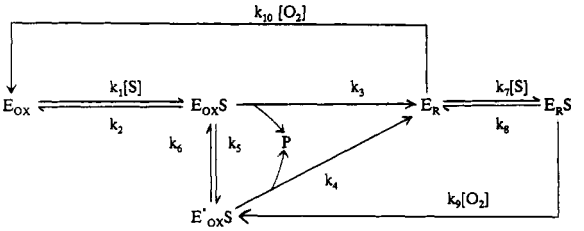

mechanism which could reconcile the data obtained for MTHS. Computer simulations based on Scheme IIB (Figure 7B) agreed well with the experimental data. The distribution of the enzyme species in the simulation was particularly sensitive to changes in the step for binding of substrate to the reduced enzyme and to a lesser extent to the equilibrium $E_{OX}S \rightleftharpoons E^*_{OX}S$. This latter step is not identified by the experiments described here. Two possible scenarios could explain the kinetic effects. Either oxygen binds to the $E_{OX}S$ complex before reduction takes place and the presence of oxygen in the complex stimulates reduction, or the $E_{OX}S$ complex can isomerize slowly to a transition state, $E^*_{OX}S$, in which the flavin is more rapidly reduced. The latter species could be the product of the reoxidation of E_RS

$$E_RS + O_2 \rightarrow E^*_{OX}S + H_2O_2$$

so that, in turnover experiments, the slow reduction and the slow isomerization of $E_{OX}S \rightleftharpoons E^*_{OX}S$ would be bypassed.

Figure 7 shows theoretical curves generated from Scheme II using the individual rate constants and K_D values known for MPTP (Figure 7A) and MTHS (Figure 7B). The theoretical curve for MTHS mimics well the curvature obtained experimentally. The parameters describing the curve are very sensitive to changes in k_7 and k_8 which define the binding of substrate to the reduced enzyme. When k_7 and k_8 are replaced by a rapid equilibrium step, the theoretical double-reciprocal plot becomes linear (not shown). Interestingly, the theoretical double-reciprocal plot for MPTP does show a little curvature, but only at very high MPTP concentrations (>20 mM). Such high concentrations (200 K_m) have not been used by us experimentally. The particular set of conditions offered by the oxidation of MTHS by MAO A has been critical in bringing the potential curvature due to the branched pathway into the range of experimental observation.

DISCUSSION

Curvature in double-reciprocal plots can arise for many reasons. In the first paper, (Sablin *et al.*, 1990) in which a crude enzyme preparation was used, contributions to the oxidation by two enzymes (MAO A and B) could not be ruled out. However, the curve in Figure 1 was obtained with pure MAO A. In contrast, the oxidation of *trans*-MTHS by pure MAO B was linear (data not shown). A second concern in seeking an explanation of the curvature was the facile photoinduced conversion of *trans*-MTHS to *cis*-MTHS. The experiments were performed carefully using fresh solutions kept dark at all times. In addition, we have found that not just the oxidation of MTHS but the oxidation of all MTHS derivatives gave curved plots, and furthermore both the *cis* and *trans* forms of each showed similar kinetics (S. O. Sablin, M. J. Krueger, T. P. Singer, S. O. Bachurin, A. B. Kharei, S. M. N. Efange, and S. E. Tkachenko, unpublished results). This means that these alternate possibilities can be eliminated.

The simulations based on Scheme IIA demonstrate that the branched pathway can give rise to both linear and nonlinear double-reciprocal patterns, depending on the rate and binding constants for the substrate. Several conditions must be fulfilled to observe such curvature. First, the rate of reoxidation of the reduced enzyme must be stimulated by substrate; i.e., $E_RS \rightarrow E_{OX}S$ is markedly faster than $E_R \rightarrow E_{OX}$. This is true for all MAO A substrates examined so far but only selected B substrates. Stimulation of the rate of oxidation by a given substrate is greater with MAO A than with MAO B (Tan & Ramsay, 1993). The ratio of the rates of oxidation of E_RS and E_R may influence the ability to detect the effects in the steady state. If the substrate stimulates the rate of oxidation only 6-fold (e.g., serotonin), deviation from linearity would be difficult to detect. If the substrate stimulates oxidation strongly (e.g., kynuramine), the E_RS pathway would be predominant within the experimentally feasible conditions. Second, binding of the substrate to the reduced enzyme must be slow. For MTHS, the difference between Figures 5A and 6 shows that the rate of binding is between the rates of oxidation of E_R and E_RS. For MPTP, the rate of binding to E_R is slower than the rate of reoxidation of the free enzyme because MPTP mixed with reduced enzyme at the same time as oxygen does not stimulate the rate of oxidation above that of the free enzyme. In the computer simulations, the values set for k_7 and k_8 (Scheme II) had a strong influence on the curvature of the steady-state Lineweaver–Burk plot. When $E_R \rightleftharpoons E_RS$ was set to a rapid equilibrium step, no curvature was obtained. Third, the reductive rate (k_3) should be of the same order as the rate of reoxidation of free enzyme (k_{10} in Scheme II). The k_3 for $E_{OX}S \rightarrow E_RP$ is 0.2 s^{-1} for MPTP compared to k_{10}, which is 1 s^{-1}. All MAO A substrates give k_3 values below 3 s^{-1} (Tan & Ramsay, 1993). Additionally, for MTHS, the proposed alternative pathway in the reductive half-reaction ($E^*_{OX}S$) provides another variable influencing the curvature. The rate (k_5) of the isomerization step, $E_{OX}S \rightarrow E^*_{OX}S$, has a strong influence on the low K_m part of the plot, i.e., on the slope of the double-reciprocal plot at low substrate concentration.

MTHS and its analogs provide a combination of conditions which permits the demonstration in the steady state of the consequences of the branched pathway mechanism proposed for MAO (Ramsay *et al.*, 1987; Ramsay, 1991).

REFERENCES

Altomare, C., Carrupt, P. A., Gaillard, P., El Tayar, N., Testa, B., & Carotti, A. (1992) *Chem. Res. Toxicol. 5*, 366–375.

Efange, S. M. N., & Boudreau, R. J. (1991) *J. Comput.-Aided Mol. Des. 5*, 405–417.

Husain, M., Edmondson, D. E., & Singer, T. P. (1982) *Biochemistry 21*, 595–600.

Kim, J. M., Cho, I. S., & Mariano, P. S. (1991) *J. Org. Chem. 56*, 4943–4953.

Massey, V. (1991) in *Flavins and Flavoproteins* (Curti, B., Ronchi, S., & Zanetti, G., Eds.) pp 59–66, de Gruyter, Berlin.

Massey, V., Schopfer, L. M., & Anderson, R. F. (1988) in *Oxidases and Related Redox Systems* (King, T. E., Mason,

H. S., & Morrison, M., Eds.) pp 147–166, Liss, New York.
Nagy, J., & Salach, J. I. (1981) *Arch. Biochem. Biophys. 208*, 388–394.
Ramsay, R. R. (1991) *Biochemistry 30*, 4624–4629.
Ramsay, R. R., Koerber, S. C., & Singer, T. P. (1987) *Biochemistry 26*, 3045–3050.
Ramsay, R. R., Tan, A. K., & Weyler, W. (1992) *J. Neural. Transm.* (in press).
Sablin, S. O. (1991) Ph.D. dissertation, M. Gorky Library, M. V. Lomonosov Moscow State University, Moscow.
Sablin, S. O., Bachurin, S. O., & Tkachenko, S. E. (1990) *J. Neural. Transm., Suppl. 32*, 119–122.
Silverman, R. B., Hoffman, S. J., & Catus, W. B., III (1980) *J. Am. Chem. Soc. 102*, 7126–7128.
Singer, T. P. (1991) in *Chemistry and Biochemistry of Flavoenzymes* (Muller, F., Ed.) Vol. III, pp 437–470, CRC Press, Boca Raton, FL.
Tan, A. K., & Ramsay, R. R. (1993) *Biochemistry 32*, 2137–2143.
Tan, A. K., Weyler, W., Salach, J. I., & Singer, T. P. (1991) *Biochem. Biophys. Res. Commun. 181*, 1084–1088.
Youngster, S. K., McKeown, K. A., Jin, Y.-Z., Ramsay, R. R., Heikkila, R. E., & Singer, T. P. (1989) *J. Neurochem. 53*, 1837–1842.